RSC Advances

PAPER

View Article Online
View Journal | View Issue

Cite this: *RSC Adv.*, 2020, **10**, 30683

Synthesis and biological activity evaluation of azacycloheptane sulfonamide derivatives as potential orexin receptor antagonists†

Bin Guo, [a] Jingya Xiu, [b] Yi Shen[b] and Qingeng Li*[a]

Received 9th June 2020
Accepted 12th August 2020

DOI: 10.1039/d0ra05068g

rsc.li/rsc-advances

As the orexin signaling system is crucial for the regulation of the sleep/wake cycle, inhibitors of orexin-1 and orexin-2 receptors are of significant interest in the treatment of insomnia. Herein, a series of novel azacycloheptane sulfonamide derivatives were designed and synthesized, and all the compounds were evaluated as potential orexin receptor inhibitors by FLIPR Tetra calcium assay. A majority of the tested azacycloheptane sulfonamide derivatives showed OX1R and OX2R inhibitory activity. Chloro-substituted derivatives functionalized at the C5 or C6 position of the benzoxazole group exhibited better inhibitory activity for OX1R and OX2R than unsubstituted derivatives functionalized at C5 or C6. In addition, phenyl group modification had positive effects on the inhibitory activities, and an electron-withdrawing fluorine group at the *ortho* or *meta* position of the phenyl ring improved the OX2R inhibitory activity of the derivatives. This suggests that azacycloheptane sulfonamide derivatives are promising scaffolds for the development of OX1R and OX2R antagonists.

Introduction

Orexin-1 (OX1R) and orexin-2 (OX2R) receptors are G-protein coupled receptors (GPCRs) that were discovered in 1998.[1,2] Many studies have confirmed that orexin signaling system is crucial for the regulation of the sleep/wake cycle.[3,4] Orexin peptide-deficient mice and humans with narcolepsy have similar symptoms.[5] Moreover, mice with knockout of OX1R and OX2R showed an acute narcoleptic phenotype similar to peptide-deficient animals.[6] Consistent with these observations, rats treated with orexin peptides by direct intracerebroventricular (ICV) infusions showed an increase in arousal and a decrease in sleep.[7] As a result, due to their intimate involvement in insomnia diseases, orexin receptors have become promising drug targets for treating insomnia.[8–13]

A number of antagonists of OX1R and OX2R, such as selective orexin-1 receptor antagonists (1-SORAs), selective orexin-2 receptor antagonists (2-SORAs) and dual orexin receptor antagonists (DORAs), have been synthesized in the past decade.[14–22] However, many studies have found that a more robust effect on increases REM and non-REM sleep when both receptors are inhibited.[6] So, most work has focused on DORAs. Almorexant, developed by Actelion and GlaxoSmithKline, was the first DORA, and it initially showed positive effects in the treatment of insomnia symptoms.[23,24] However, almorexant was ultimately discontinued in 2011 because of safety concerns.[10] The best dual orexin antagonists reported to date are suvorexant and lemborexant, which received approval from the FDA in 2014 and 2019, respectively.[25–29] Despite these advances and the results of orexin antagonists, adverse effects such as somnolence limit the application of orexin antagonists as first-line treatments for insomnia. Therefore, further studies are needed to identify selective orexin antagonists and dual orexin antagonists for potential use as sleep drugs.

In this study, we designed and synthesized a series of twenty one novel azacycloheptane sulfonamide derivatives. The *in vitro* OX1R and OX2R inhibitory activities were assayed to evaluate the potential of these compounds as orexin antagonists. Compound **23** showed the most potent activities in both the OX1R and OX2R inhibition assays. The structure–activity analysis of these compounds was conducted according to their biological activities *in vitro*. Then, molecular docking simulations were performed to elucidate the binding mode of active compound **23**. To the best of our knowledge, this is the first report on azacycloheptane sulfonamide derivatives with potent inhibitory activities against OX1R and OX2R.

Results and discussion

Chemistry

The synthetic strategy for the prepare of target compounds **9–29** are depicted in Scheme 1. Using benzylglycine and (*R*)-3-aminobutanoic acid as starting materials, intermediate products **1**

[a]*School of Pharmaceutical Science, Chongqing Medical University, Chongqing 400016, China. E-mail: 13908387568@vip.163.com*

[b]*Jiangsu Nhwaluokang Pharmaceutical Research and Development Co., Ltd., Chongqing 400016, China*

† Electronic supplementary information (ESI) available. See DOI: 10.1039/d0ra05068g

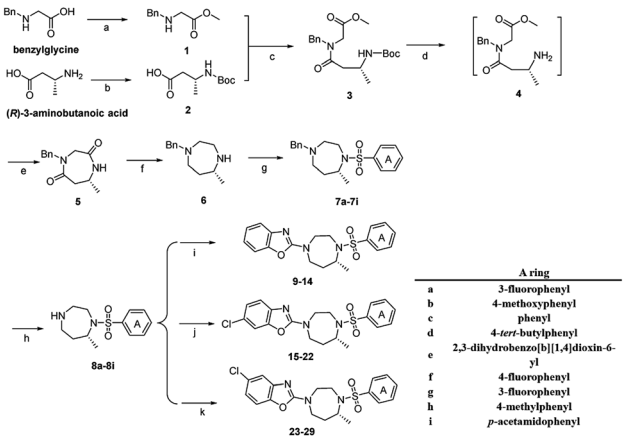

Scheme 1 Synthesis of the azacycloheptane sulfonamide derivatives **9–29**. Reagents and conditions: (a) methanol, thionyl chloride, rt, 3 days; (b) 1,4-dioxane, H_2O, sodium hydroxide, di-*tert*-butyl dicarbonate, rt, 3 days; (c) EDCI, HOBt, triethylamine, DMF, 0–5 °C; (d) hydrochloric acid, ethyl acetate, methanol, rt, 3 h; (e) sodium methoxide, methanol, rt, 0.5 h; (f) LAH, tetrahydrofuran, 0–5 °C; (g) triethylamine, DCM, rt, 1 h; (h) 10% Pd/C, methanol, 24 h; (i) 2-chlorobenzoxazole, potassium carbonate, DMF, 60 °C, 3 h. (j) 2,6-Dichlorobenzoxazole, potassium carbonate, DMF, 60 °C, 3 h. (k) 2,5-Dichlorobenzoxazole, potassium carbonate, DMF, 60 °C, 3 h.

and **2** were constructed. The reaction between **1** and **2** in the presence of 1-hydroxybenzotriazole (HOBt) and 1-ethyl-3-(3-dimethylaminopropyl)carbodiimide hydrochloride (EDCI) proceeded at 0–5 °C and afforded compound **3**. Treatment of **3** with hydrochloric acid in ethyl acetate at room temperature generated compound **4**, which was directly treated with sodium methoxide to obtain compound **5**. Compound **6** was obtained from the reaction of compound **5** with lithium aluminium hydride (LAH) in tetrahydrofuran (THF). Then, compound **6** was reacted with a series of substituted benzenesulfonyl chloride derivatives in dichloromethane (DCM) to afford compounds **7a–7i**. Compounds **7a–7i** were reduced to the corresponding secondary amines with hydrogen to provide compounds **8a–8i**. Finally, target compounds **9–29** were synthesized by reacting compounds **8a–8i** with the corresponding chlorine-substituted benzoxazole derivatives in *N*,*N*-dimethylformamide (DMF) at 55–60 °C. The structures of compounds **1, 2, 5, 6, 7a–7i,** and **8a–8i** were qualitatively confirmed by mass spectrometry (MS). The structures of compounds **9–29** were confirmed by ^{1}H and ^{13}C NMR spectroscopy and HRMS.

Biological activity and *in vitro* SAR

The inhibitory activities of compounds **9–29** for OX1R and OX2R were tested using a previously described FLIPR Tetra calcium assay (Tables 1–3). The IC_{50} values of suvorexant against OX1R and OX2R are 0.14 μM and 0.15 μM, respectively. A majority of the tested azacycloheptane sulfonamide derivatives showed OX1R and OX2R inhibitory activities. Furthermore, compound **23** showed much more potent combined inhibitory activities for OX1R (IC_{50} = 0.63) and OX2R (IC_{50} = 0.17 μM) than did the other compounds, and its potency is

Table 1 The IC_{50} values of the prepared compounds **9–14** against OX1R and OX2R: part 1

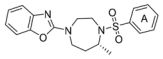

Compd	A-Ring	IC_{50} (μM) OX1R	OX2R
9	3-Fluorophenyl	NA[a]	3.80
10	4-Methoxyphenyl	NA[a]	NA[a]
11	4-*tert*-Butylphenyl	NA[a]	1.77
12	2,3-Dihydrobenzo[*b*][1,4]dioxin-6-yl	NA[a]	NA[a]
13	4-Fluorophenyl	NA[a]	NA[a]
14	4-Methylphenyl	NA[a]	1.79
Suvorexant	—	0.14	0.15

[a] No inhibitory activity.

comparable to that of suvorexant. The OX1R inhibitory activities of compounds **19, 24** and **25** are similar to that of suvorexant. However, the OX1R (IC_{50} = NA) and OX2R (IC_{50} = NA) inhibitory activities shown by compounds **10, 12** and **13,** which contained 4-methoxyphenyl, 2,3-dihydrobenzo[*b*][1,4]dioxin-6-yl, or 4-fluorophenyl, were not observed.

Structure–activity analysis revealed that a chloro substituent at the C5 or C6 position of the benzoxazole group plays a key role in the inhibitory activities of these azacycloheptane sulfonamide derivatives for OX1R and OX2R. In general, the derivatives with 6-dichlorobenzoxazole group (**15–22**) or 5-dichlorobenzoxazole (**23–29**) group showed better OX1R and OX2R inhibitory activities than the derivatives with unsubstituted benzoxazole group (**9–14**). The inhibitory activities of the derivatives with benzoxazole group and various substituted phenyl groups, such as 3-fluorophenyl (**9**), 4-methoxyphenyl (**10**), 4-*tert*-butylphenyl (**11**), 2,3-dihydrobenzo[*b*][1,4]dioxin-6-yl (**12**), 4-fluorophenyl (**13**) or *p*-methylphenyl (**14**) for OX1R and

Table 2 The IC_{50} values of the prepared compounds **15–22** against OX1R and OX2R: part 2

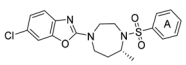

Compd	A-Ring	IC_{50} (μM) OX1R	OX2R
15	3-Fluorophenyl	1.98	1.65
16	4-Methoxyphenyl	2.29	5.11
17	Phenyl	8.58	1.52
18	4-*tert*-Butylphenyl	NA[a]	1.32
19	2,3-Dihydrobenzo[*b*][1,4]dioxin-6-yl	0.20	1.78
20	4-Fluorophenyl	NA[a]	NA[a]
21	2-Fluorophenyl	NA[a]	3.87
22	*p*-Acetamidophenyl	1.33	2.05
Suvorexant	—	0.14	0.15

[a] No inhibitory activity.

Table 3 The IC_{50} values of the prepared compounds **23–29** against OX1R and OX2R: part 3

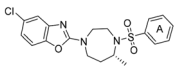

Compd	A-Ring	IC_{50} (μM) OX1R	OX2R
23	3-Fluorophenyl	0.63	0.17
24	4-Methoxyphenyl	0.21	1.80
25	Phenyl	0.57	1.09
26	4-*tert*-Butylphenyl	NA[a]	1.15
27	2,3-Dihydrobenzo[*b*][1,4]dioxin-6-yl	0.75	1.20
28	2-Fluorophenyl	1.58	1.48
29	*p*-Acetamidophenyl	4.52	4.89
Suvorexant	—	0.14	0.15

[a] No inhibitory activity.

OX2R were very weak or could hardly be observed. Analysis **15–17**, **19**, and **22–29**, with chloro substituents at the C5 or C6 position, revealed remarkably enhanced inhibitory activities for these derivatives against OX1R, and their affinities for OX2R also changed. Compared to the best OX2R inhibitor, C5 and C6 unsubstituted **11**, most of the chloro-substituted compounds (**15**, **17–18**, **23**, and **25–28**) showed improved inhibitory activities against OX2R. The evaluation of the derivatives with chloro-substituted benzoxazole groups and substituted phenyl groups, *i.e.*, *p*-methoxyphenyl **16**, *p*-acetamidophenyl **22**, *p*-methoxyphenyl **24** and *p*-acetamidophenyl **29**, revealed that the electron-donating groups 4-methoxyphenyl and *p*-acetamidophenyl at the *para* position of the phenyl ring decreased the inhibitory activity for OX2R. In general, an electron-withdrawing fluorine group at the *ortho* or *meta* position of phenyl ring improved the inhibitory activity of the derivative for OX2R. Phenyl group modification positively impacted the inhibitory activities of these compounds. **19** and **24** were the best OX1R inhibitors, and **23** was the best OX1R and OX2R dual inhibitor.

Molecular docking

To identify the possible binding modes of our inhibitors, molecular docking of compounds **23** and **19** and suvorexant was performed to elucidate the key interactions within the active sites of OX1R and OX2R. As shown in Fig. 1, the docking of suvorexant into the binding site of OX1R indicates one key hydrogen bonding interaction between the O in the amide carbonyl and Asn318. In addition, a π–cation interaction between the substituted phenyl group and His344 was observed. The docking of compound **23** into the binding site of OX1R indicates hydrogen bonding interaction between the O in the sulfonamide and Asn318 and a cation–π interaction between the 3-fluoro-substituted phenyl group and His344. The docking of compound **19** into the binding site of OX1R indicates that a hydrogen bonding interaction between the O in the sulfonamide and Asn318 and three carbon hydrogen bonding

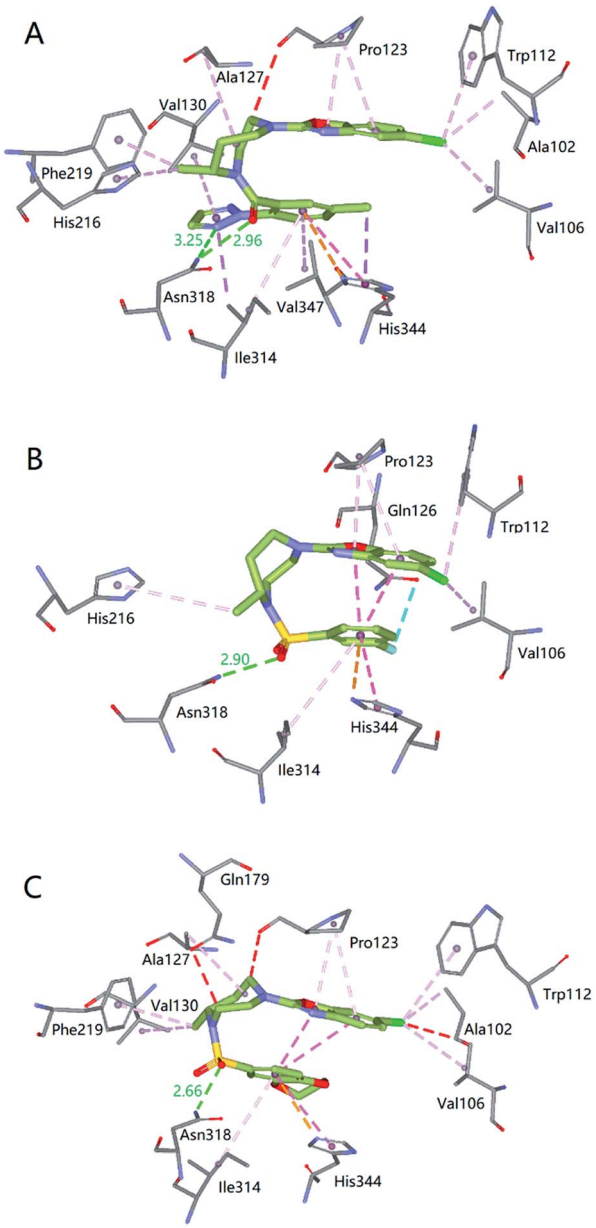

Fig. 1 (A) 3D interaction diagram of suvorexant with OX1R. (B) 3D interaction diagram of **23** with OX1R. (C) 3D interaction diagram of **19** with OX1R. Hydrogen bond interactions is represented by green bonds, hydrophobic interactions by pink bonds, π–sulfur interactions by dark blue bonds, carbon–hydrogen interactions by red bonds, π–cation interactions by dark yellow bonds, π–sigma interactions by purple bonds, π–π stacked interactions by dark pink bonds, and halogen (fluorine) interactions by light blue bonds.

interactions formed with Ala102, Gln179 and Pro123. A π–cation interaction between the substituted phenyl group and His344 was also observed. Compound **19** showed stronger OX1R inhibitory activity than did compound **23** and the other azacycloheptane sulfonamide derivatives. The possible reason is compound **19** have stronger hydrogen bond and more carbon hydrogen bonding interactions. As shown in Fig. 2, the docking of suvorexant into the binding site of OX2R indicates one key hydrogen bond between the O in the amide and Asn324 and

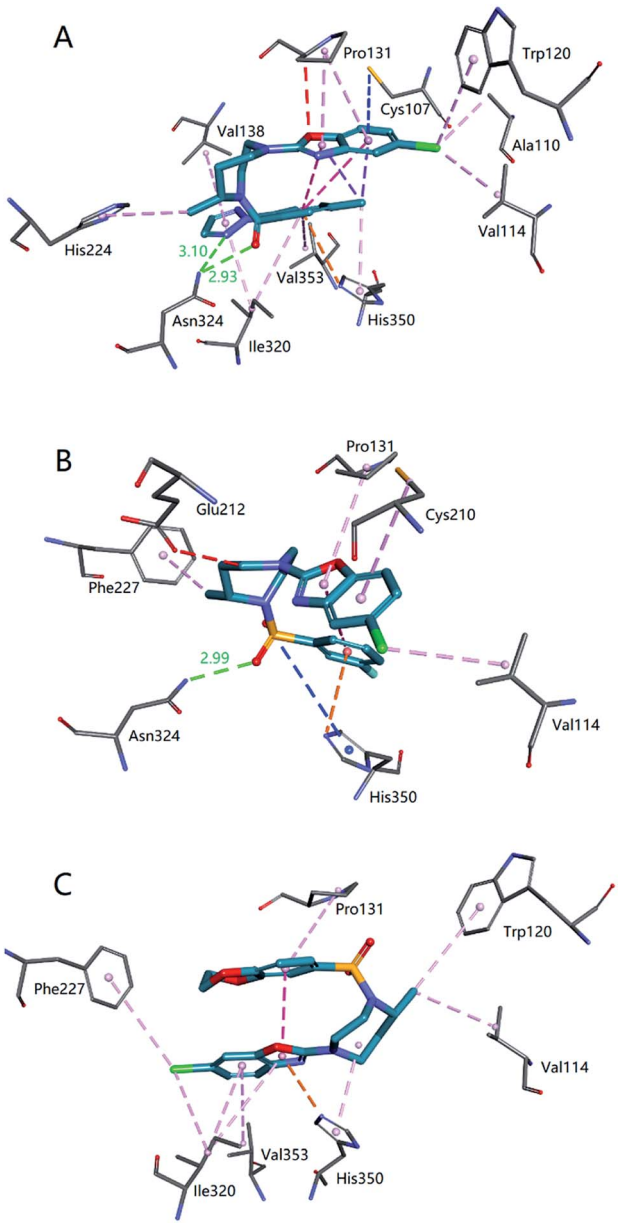

Fig. 2 (A) 3D interaction diagram of suvorexant with OX2R. (B) 3D interaction diagram of **23** with OX2R. (C) 3D interaction diagram of **19** with OX2R. Hydrogen bond interactions is represented by green bonds, hydrophobic interactions by pink bonds, π–sulfur interactions by dark blue bonds, carbon hydrogen interactions by red bonds, π–cation interactions by dark yellow bonds, π–sigma interactions by purple bonds, π–π stacked interactions by dark pink bonds, and halogen (fluorine) interactions by light blue bonds.

a π–cation interaction between the substituted phenyl group and His350. The docking of compound **23** into the binding site of OX2R indicates one key hydrogen bond between the O atoms in the sulfonamide and Asn324. Furthermore, a π–cation interaction and π–sulfur interaction were also observed. The inhibitory activity of compound **19** towards OX2R was weaker than those of suvorexant and compound **23**. The docking of compound **19** into the binding site of OX2R showed that the key hydrogen bond between the O in the sulfonamide and Asn324 was absent. Compared to compound **23** and suvorexant, compound **19** shows completely different docking behavior for OX2R. The possible reason is that the sterically hindered of 2,3-dihydrobenzo[*b*][1,4]dioxin-6-yl is larger than other substituent groups. More importantly, the substituent and the benzene ring are rigidly connected. In summary, the result of molecular docking are in agreement with the experimental activity result that the OX2R inhibitory activity of compound **23** (IC_{50} = 0.17 μM) is comparable to that of suvorexant (IC_{50} = 0.15 μM), but the inhibitory activity of **23** (IC_{50} = 0.63 μM) for OX1R was slightly weaker than that of suvorexant (IC_{50} = 0.14 μM).

Experimental section

General information

Reagents (Energy Chemical, Shanghai, China) were used without further purification. Preparative TLC separations were performed using silica gel GF254 (Qingdao Hailang Chemical, Qingdao, China). NMR spectra were recorded on a Bruker Av500M spectrometer and a Bruker ARX 600 MHz spectrometer (Bruker, Zurich, Swiss), and TMS was used as the internal standard. MS data were obtained on a Waters ACQUITY QDa. HRMS data were obtained on a Bruker impact II O-TOF mass spectrometry. If necessary, organic solvents were dried by standard methods before use.

Chemistry

Starting compounds **1–3** were synthesized according to previously reported methods as given below.[30,31]

Synthesis of (*R*)-4-benzyl-7-methyl-1,4-diazepane-2,5-dione (5). To a solution of methyl (*R*)-*N*-benzyl-*N*-(3-((*tert*-butoxycarbonyl)amino)butanoyl)glycinate (**3**) (20.00 g, 54.9 mmol) in 200 ml of ethyl acetate (180 ml) and methanol (20 ml) was slowly introduced freshly prepared hydrochloric acid with stirring. The reaction mixture was stirred at rt for 3 h. Ethyl acetate and methanol were removed under vacuum. The residue was dissolved and then concentrated to dryness under vacuum 3 times. The obtained residue was immediately taken on to the next step. To a solution of the obtained residue in 160 ml of CH_3OH was added sodium methoxide (19.27 g, 356.7 mmol). The reaction mixture was stirred at rt for 0.5 h. The reaction mixture was cooled to 0–5 °C and quenched with 320 ml of water. The mixture was extracted with CH_2Cl_2, and the organic layers were combined, washed with water and then bine, dried over $MgSO_4$ and concentrated to provide compound **5** (10.7 g, white solid, yield: 83.9%). MS (ESI^+) *m*/*z* calculated for $C_{13}H_{16}N_2O_2$ $[M + H]^+$ 233.12, found 233.10.

Synthesis of (*R*)-1-benzyl-5-methyl-1,4-diazepane (6). A solution of (*R*)-4-benzyl-7-methyl-1,4-diazepane-2,5-dione (**5**) (4.20 g, 120.45 mmol) in THF (42 ml) was added dropwise to a solution of LAH (34.85 ml, 87.11 mmol) in dry THF (21 ml) cooled to 0–5 °C. After stirring at rt overnight, the reaction was cooled to 0–5 °C and quenched with water (1.5 ml), then 15% NaOH solution (1.5 ml) followed by an additional 4.5 ml of water. The mixture was dried with $MgSO_4$ and stirred for 0.5 h. The filtrate was concentrated under vacuum to provide **6** (3.1 g, light-yellow

oil, yield: 83.9%). MS (ESI$^+$): *m*/*z* calculated for $[M + H]^+$ 205.16, found 205.12.

General procedure for the preparation of compounds 7a–7i. A mixture of **6** (1.00 g, 4.89 mmol), the appropriate substituted benzenesulfonyl chloride derivative (4.16 mmol) and triethylamine (9.78 mmol) in DCM was stirred at rt for 1 h. Then, the reaction mixture was washed with water and brine, dried over Na_2SO_4, filtered, and concentrated under vacuum to afford compounds **7a–7i**. The obtained compounds (**7a–7i**) were immediately taken into the next step without purification. The structures of compounds **7a–7i** were confirmed by MS.

General procedure for the preparation of compounds 8a–8i. Compounds **7a–7i** (4.89 mmol) were dissolved in methanol (10 ml). After adding a portion of 10% Pd/C (100 mg), the reaction was stirred for 24 h under a H_2 atmosphere at rt. The reaction mixture was filtered, and the filtrate was concentrated under vacuum to provide **8a–8i**. The obtained compounds were immediately taken into the next step without purification. The structures of compounds **8a–8i** were confirmed by MS.

General procedure for the preparation of compounds 9–14. A mixture of compounds **8a**, **8b–8f**, or **8h** (1.77 mmol), 2-chlorobenzoxazole (1.42 mmol) and potassium carbonate (2.30 mmol) was dissolved in DMF (7.5 ml). The mixture was stirred at 60 °C for 3 h. The reaction was then quenched with water, and the mixture was extracted with ethyl acetate. The organic layers were combined and washed with water and then bine, dried over $MgSO_4$ and concentrated under vacuum. The residue was purified by preparative TLC and then recrystallized from petroleum ether (60–90) to afford **9–14**.

9. Yield: 42.5%, off-white solid; ^{1}H NMR (500 MHz, $CDCl_3$) δ 7.61 (d, $J = 7.7$ Hz, 1H), 7.54 (d, $J = 7.4$ Hz, 1H), 7.48–7.39 (m, 1H), 7.34 (d, $J = 7.8$ Hz, 1H), 7.26 (s, 1H), 7.22–7.12 (m, 2H), 7.02 (t, $J = 7.7$ Hz, 1H), 4.27 (dd, $J = 13.4$, 6.6 Hz, 1H), 4.13 (d, $J = 14.7$ Hz, 1H), 4.06–3.98 (m, 1H), 3.94 (d, $J = 15.1$ Hz, 1H), 3.68–3.59 (m, 1H), 3.52 (dd, $J = 14.6$, 7.7 Hz, 1H), 3.36–3.24 (m, 1H), 2.37–2.23 (m, 1H), 1.73 (dd, $J = 15.1$, 7.6 Hz, 1H), 1.01 (d, $J = 6.7$ Hz, 3H); ^{13}C NMR (151 MHz, DMSO-d_6) δ: 163.10, 162.02, 161.46, 148.93, 143.68, 132.19, 124.33, 123.23, 120.62, 120.24, 116.07, 114.22, 114.06, 109.27, 51.69, 48.81, 44.03, 42.82, 34.87, 17.85; HRMS (ESI (+)) *m*/*z* calculated for $C_{19}H_{20}FN_3O_3S$ $[M + H]^+$: 390.1282, found 390.1291.

10. Yield: 48.2%, off-white solid; ^{1}H NMR (500 MHz, $CDCl_3$) δ 7.74 (d, $J = 8.6$ Hz, 2H), 7.34 (d, $J = 7.7$ Hz, 1H), 7.24 (d, $J = 7.9$ Hz, 1H), 7.16 (t, $J = 7.6$ Hz, 1H), 7.01 (t, $J = 7.7$ Hz, 1H), 6.89 (d, $J = 8.6$ Hz, 2H), 4.24 (dd, $J = 13.2$, 6.5 Hz, 1H), 4.09 (d, $J = 14.3$ Hz, 1H), 3.97 (t, $J = 18.4$ Hz, 2H), 3.78 (s, 3H), 3.62 (t, $J = 12.3$ Hz, 1H), 3.50 (dd, $J = 14.4$, 7.6 Hz, 1H), 3.31–3.19 (m, 1H), 2.30–2.19 (m, 1H), 1.69 (d, $J = 5.1$ Hz, 1H), 1.00 (d, $J = 6.6$ Hz, 3H); ^{13}C NMR (151 MHz, DMSO-d_6) δ: 162.72, 162.06, 148.93, 143.73, 133.09, 129.20, 124.32, 120.59, 116.04, 114.86, 109.25, 56.00, 51.16, 48.73, 43.94, 42.40, 34.86, 17.88; HRMS (ESI (+)) *m*/*z* calculated for $C_{20}H_{23}N_3O_4S$ $[M + H]^+$: 402.1482, found 402.1481.

11. Yield: 31.9%, white solid; ^{1}H NMR (500 MHz, $CDCl_3$) δ 7.74 (d, $J = 7.8$ Hz, 2H), 7.45 (d, $J = 7.6$ Hz, 2H), 7.34 (d, $J = 7.7$ Hz, 1H), 7.26 (d, $J = 6.4$ Hz, 1H), 7.16 (t, $J = 7.6$ Hz, 1H), 7.01 (t, $J = 7.7$ Hz, 1H), 4.25 (d, $J = 6.7$ Hz, 1H), 4.13 (d, $J = 14.2$ Hz, 1H), 4.06–3.91 (m, 2H), 3.69–3.59 (m, 1H), 3.50 (dd, $J = 14.4$, 7.5 Hz, 1H), 3.32–3.22 (m, 1H), 2.30–2.20 (m, 1H), 1.75–1.67 (m, 1H), 1.31 (d, $J = 18.8$ Hz, 9H), 1.00 (d, $J = 6.4$ Hz, 3H); ^{13}C NMR (151 MHz, DMSO-d_6) δ: 162.05, 156.16, 148.94, 143.73, 138.52, 126.92, 126.52, 124.33, 120.59, 116.06, 109.26, 51.22, 48.82, 43.80, 42.46, 35.21, 34.88, 31.16, 17.85; HRMS (ESI (+)) *m*/*z* calculated for $C_{23}H_{29}N_3O_3S$ $[M + H]^+$: 428.2002, found 428.2001.

12. Yield: 35.7%, white solid; ^{1}H NMR (600 MHz, $CDCl_3$) δ: 7.38 (s, 1H), 7.36–7.29 (m, 2H), 7.26–7.22 (m, 1H), 7.18 (d, $J = 6.7$ Hz, 1H), 7.04 (d, $J = 6.7$ Hz, 1H), 6.89 (d, $J = 8.0$ Hz, 1H), 4.23 (d, $J = 12.8$ Hz, 4H), 4.12 (d, $J = 12.2$ Hz, 1H), 4.04 (d, $J = 7.8$ Hz, 1H), 3.94 (d, $J = 15.0$ Hz, 1H), 3.63 (d, $J = 12.0$ Hz, 1H), 3.54 (s, 1H), 3.32–3.19 (m, 1H), 2.28 (d, $J = 6.3$ Hz, 1H), 1.76–1.64 (m, 1H), 1.26 (s, 1H), 1.02 (d, $J = 5.8$ Hz, 3H); ^{13}C NMR (151 MHz, $CDCl_3$) δ: 161.19, 148.45, 147.25, 143.59, 133.75, 124.35, 121.01, 120.54, 117.78, 116.44, 115.95, 108.93, 64.46, 64.14, 51.31, 49.57, 44.99, 43.52, 35.52, 18.32; HRMS (ESI (+)) *m*/*z* calculated for $C_{21}H_{23}N_3O_5S$ $[M + H]^+$: 430.1431, found 430.1430.

13. Yield: 40.8%, white solid; ^{1}H NMR (500 MHz, $CDCl_3$) δ 7.83 (s, 2H), 7.34 (d, $J = 7.6$ Hz, 1H), 7.30–7.21 (m, 1H), 7.14 (dt, $J = 15.5$, 7.4 Hz, 3H), 7.02 (t, $J = 7.5$ Hz, 1H), 4.24 (d, $J = 6.6$ Hz, 1H), 4.12 (d, $J = 14.3$ Hz, 1H), 4.06–3.88 (m, 2H), 3.64 (dd, $J = 13.3$, 11.1 Hz, 1H), 3.52 (dd, $J = 14.5$, 7.6 Hz, 1H), 3.33–3.23 (m, 1H), 2.36–2.20 (m, 1H), 1.73 (s, 1H), 1.00 (d, $J = 6.4$ Hz, 3H); ^{13}C NMR (151 MHz, DMSO-d_6) δ: 165.47, 163.81, 162.02, 148.92, 143.67, 137.84, 130.06, 129.82, 126.98, 124.34, 120.64, 117.00, 116.85, 116.06, 109.26, 51.50, 48.76, 44.04, 42.68, 34.84, 17.86; HRMS (ESI (+)) *m*/*z* calculated for $C_{19}H_{20}FN_3O_3S$ $[M + H]^+$: 390.1282, found 390.1281.

14. Yield: 45.3%, white solid; ^{1}H NMR (500 MHz, $CDCl_3$) δ 7.74 (s, 2H), 7.37 (s, 1H), 7.29 (d, $J = 20.4$ Hz, 3H), 7.21 (s, 1H), 7.06 (s, 1H), 4.30 (s, 1H), 4.13 (d, $J = 14.0$ Hz, 1H), 4.01 (d, $J = 14.2$ Hz, 2H), 3.66 (t, $J = 11.6$ Hz, 1H), 3.53 (s, 1H), 3.30 (t, $J = 12.0$ Hz, 1H), 2.38 (s, 3H), 2.29 (s, 1H), 1.72 (s, 1H), 1.04 (s, 3H); ^{13}C NMR (151 MHz, DMSO-d_6) δ: 162.01, 148.92, 143.71, 143.37, 138.58, 130.19, 126.98, 124.31, 120.59, 116.04, 109.25, 51.27, 48.62, 43.90, 42.43, 34.76, 21.29, 17.91; HRMS (ESI (+)) *m*/*z* calculated for $C_{20}H_{23}N_3O_3S$ $[M + H]^+$: 386.1533, found 386.1532.

General procedure for the preparation of compounds 15–22. A mixture of compound **8a–8g**, or **8i** (1.77 mmol), 2,6-dichlorobenzoxazole (1.42 mmol) and potassium carbonate (2.30 mmol) was dissolved in DMF (7.5 ml). The mixture was stirred at 60 °C for 3 h. Then, the reaction was quenched with water, and the mixture was extracted with ethyl acetate. The organic layers were combined, washed with water and then bine, dried over $MgSO_4$ and concentrated under vacuum. The residue was purified by preparative TLC and then recrystallized from petroleum ether (60–90) to afford **15–22**.

15. Yield: 41.1%, white solid; ^{1}H NMR (500 MHz, $CDCl_3$) δ 7.61 (d, $J = 7.6$ Hz, 1H), 7.54 (d, $J = 7.9$ Hz, 1H), 7.44 (dt, $J = 13.2$, 6.7 Hz, 1H), 7.32–7.18 (m, 3H), 7.14 (d, $J = 8.3$ Hz, 1H), 4.27 (dd, $J = 13.2$, 6.6 Hz, 1H), 4.09 (d, $J = 14.3$ Hz, 1H), 4.03–3.90 (m, 2H), 3.64 (dd, $J = 13.5$, 11.1 Hz, 1H), 3.52 (dd, $J = 14.5$, 7.6 Hz, 1H), 3.35–3.23 (m, 1H), 2.28 (dd, $J = 14.6$, 6.8 Hz, 1H), 1.73 (dd, $J = 15.2$, 7.6 Hz, 1H), 0.99 (t, $J = 13.2$ Hz, 3H); ^{13}C NMR (151 MHz, DMSO-d_6) δ: 163.10, 162.54, 161.45, 149.20, 143.47, 142.85, 132.19, 124.42, 123.22, 120.31, 120.17, 116.68, 114.20, 114.04,

109.94, 51.65, 48.79, 44.07, 42.60, 34.71, 17.82; HRMS (ESI (+)) m/z calculated for $C_{19}H_{19}ClFN_3O_3S$ $[M + H]^+$: 424.0892, found 424.0885.

16. Yield: 39.8%, white solid; ^{1}H NMR (500 MHz, $CDCl_3$) δ 7.74 (d, J = 8.7 Hz, 2H), 7.22 (d, J = 14.8 Hz, 2H), 7.14 (d, J = 8.3 Hz, 1H), 6.89 (d, J = 8.7 Hz, 2H), 4.30–4.19 (m, 1H), 4.05 (d, J = 14.3 Hz, 1H), 3.95 (d, J = 14.7 Hz, 2H), 3.78 (d, J = 15.2 Hz, 3H), 3.62 (t, J = 12.4 Hz, 1H), 3.51 (dd, J = 14.5, 7.7 Hz, 1H), 3.30–3.20 (m, 1H), 2.31–2.19 (m, 1H), 1.66 (dd, J = 16.0, 8.4 Hz, 1H), 1.01 (d, J = 6.6 Hz, 3H); ^{13}C NMR (151 MHz, DMSO-d_6) δ: 162.70, 162.56, 149.19, 142.88, 133.09, 129.17, 124.40, 116.62, 114.84, 109.93, 55.97, 51.12, 48.63, 43.95, 42.15, 34.67, 17.90; HRMS (ESI (+)) m/z calculated for $C_{20}H_{22}ClN_3O_4S$ $[M + H]^+$: 436.1092, found 436.1091.

17. Yield: 37.3%, white solid; ^{1}H NMR (500 MHz, $CDCl_3$) δ 7.82 (d, J = 7.2 Hz, 2H), 7.49 (dd, J = 22.5, 7.3 Hz, 3H), 7.26–7.18 (m, 2H), 7.14 (d, J = 8.2 Hz, 1H), 4.34–4.19 (m, 1H), 4.09 (d, J = 14.2 Hz, 1H), 3.98 (t, J = 14.5 Hz, 2H), 3.62 (t, J = 11.6 Hz, 1H), 3.50 (dd, J = 12.1, 7.6 Hz, 1H), 3.32–3.20 (m, 1H), 2.35–2.19 (m, 1H), 1.78–1.66 (m, 1H), 0.98 (d, J = 6.6 Hz, 3H); ^{13}C NMR (151 MHz, DMSO-d_6) δ: 162.57, 149.22, 142.88, 141.40, 133.11, 129.82, 126.97, 124.42, 116.67, 109.96, 51.41, 48.92, 44.11, 42.55, 34.82, 17.75; HRMS (ESI (+)) m/z calculated for $C_{19}H_{20}ClN_3O_3S$ $[M + H]^+$: 406.0987, found 406.0985.

18. Yield: 49.3%, white solid; ^{1}H NMR (500 MHz, $CDCl_3$) δ: 7.73 (d, J = 7.7 Hz, 2H), 7.46 (d, J = 7.7 Hz, 2H), 7.24 (dd, J = 18.9, 9.8 Hz, 2H), 7.13 (d, J = 8.3 Hz, 1H), 4.25 (d, J = 6.6 Hz, 1H), 4.09 (d, J = 14.4 Hz, 1H), 3.97 (t, J = 18.7 Hz, 2H), 3.69–3.59 (m, 1H), 3.51 (dd, J = 14.4, 7.6 Hz, 1H), 3.31–3.20 (m, 1H), 2.31–2.20 (m, 1H), 1.69 (s, 1H), 1.32 (d, J = 18.2 Hz, 9H), 1.00 (d, J = 6.5 Hz, 3H); ^{13}C NMR (151 MHz, DMSO-d_6) δ: 162.57, 156.16, 149.22, 142.90, 138.51, 126.90, 126.50, 124.43, 116.66, 109.96, 51.14, 48.77, 43.79, 42.20, 35.19, 34.71, 31.13, 17.84; HRMS (ESI (+)) m/z calculated for $C_{23}H_{28}ClN_3O_3S$ $[M + H]^+$: 462.1613, found 462.1611.

19. Yield: 29.3%, off-white solid; ^{1}H NMR (600 MHz, $CDCl_3$) δ: 7.36–7.28 (m, 2H), 7.24 (d, J = 14.3 Hz, 2H), 7.15 (d, J = 7.7 Hz, 1H), 6.89 (d, J = 8.2 Hz, 1H), 4.24 (d, J = 14.0 Hz, 4H), 4.07 (d, J = 13.7 Hz, 1H), 3.97 (dd, J = 33.5, 12.2 Hz, 2H), 3.64 (t, J = 11.4 Hz, 1H), 3.52 (t, J = 20.7 Hz, 1H), 3.30–3.19 (m, 1H), 2.33–2.20 (m, 1H), 1.73–1.64 (m, 1H), 1.26 (s, 1H), 1.00 (t, J = 16.6 Hz, 3H); ^{13}C NMR (151 MHz, $CDCl_3$) δ: 161.86, 148.80, 147.25, 143.58, 133.73, 125.86, 124.47, 120.55, 117.78, 116.37, 109.67, 64.46, 64.14, 51.25, 49.49, 44.88, 43.41, 35.47, 18.29; HRMS (ESI (+)) m/z calculated for $C_{21}H_{22}ClN_3O_5S$ $[M + H]^+$: 464.1041, found 464.1037.

20. Yield: 38.9%, white solid; ^{1}H NMR (500 MHz, $CDCl_3$) δ: 7.84 (d, J = 5.0 Hz, 2H), 7.24 (dd, J = 18.2, 9.3 Hz, 2H), 7.13 (t, J = 9.4 Hz, 3H), 4.25 (dd, J = 13.0, 6.4 Hz, 1H), 4.09 (d, J = 14.3 Hz, 1H), 4.03–3.90 (m, 2H), 3.64 (dd, J = 13.4, 11.0 Hz, 1H), 3.52 (dd, J = 14.5, 7.6 Hz, 1H), 3.31–3.21 (m, 1H), 2.34–2.23 (m, 1H), 1.71 (d, J = 7.8 Hz, 1H), 0.99 (d, J = 6.5 Hz, 3H); ^{13}C NMR (151 MHz, DMSO-d_6) δ: 165.47, 163.80, 162.53, 149.18, 142.84, 137.82, 130.04, 126.97, 124.43, 117.00, 116.85, 116.66, 109.94, 51.46, 48.71, 44.06, 42.45, 34.67, 17.86; HRMS (ESI (+)) m/z calculated for $C_{19}H_{19}ClFN_3O_3S$ $[M + H]^+$: 424.0892, found 424.0892.

21. Yield: 46.6%, light-yellow solid; ^{1}H NMR (500 MHz, $CDCl_3$) δ 7.93 (t, J = 7.4 Hz, 1H), 7.53 (d, J = 5.1 Hz, 1H), 7.33–7.20 (m, 3H), 7.15 (dd, J = 10.3, 8.6 Hz, 2H), 4.22 (dd, J = 13.3, 6.5 Hz, 1H), 4.18–3.97 (m, 3H), 3.60 (t, J = 10.8 Hz, 2H), 3.46–3.33 (m, 1H), 2.39–2.28 (m, 1H), 1.75 (s, 1H), 0.96 (d, J = 6.2 Hz, 3H); ^{13}C NMR (151 MHz, DMSO-d_6) δ: 162.59, 159.20, 157.53, 149.23, 142.88, 136.08, 130.58, 128.98, 125.58, 124.43, 117.89, 117.75, 116.69, 109.97, 51.62, 49.21, 44.26, 42.83, 34.88, 17.64; HRMS (ESI (+)) m/z calculated for $C_{19}H_{19}ClFN_3O_3S$ $[M + H]^+$: 424.0892, found 424.0891.

22. Yield: 30.5%, off-white solid; ^{1}H NMR (600 MHz, $CDCl_3$) δ: 7.73 (d, J = 7.2 Hz, 2H), 7.58 (d, J = 7.2 Hz, 2H), 7.24 (s, 2H), 7.15 (d, J = 7.6 Hz, 1H), 4.28 (d, J = 6.1 Hz, 1H), 4.01 (d, J = 13.4 Hz, 1H), 3.94 (t, J = 16.0 Hz, 2H), 3.66 (d, J = 12.2 Hz, 1H), 3.55 (s, 1H), 3.32–3.20 (m, 1H), 2.32–2.10 (m, 5H), 1.73–1.63 (m, 1H), 1.02 (d, J = 5.8 Hz, 3H); ^{13}C NMR (151 MHz, $CDCl_3$) δ: 168.60, 148.67, 141.92, 135.81, 128.01, 124.57, 119.29, 116.25, 109.74, 51.29, 49.22, 44.85, 43.10, 35.19, 24.64, 18.27; HRMS (ESI (+)) m/z calculated for $C_{21}H_{23}ClN_4O_4S$ $[M + H]^+$: 463.1201, found 463.1196.

General procedure for the preparation of compounds 23–29. A mixture of compound **8a–8c**, **8d–8g**, or **8i** (1.77 mmol), 2,5-dichlorobenzoxazole (1.42 mmol) and potassium carbonate (2.30 mmol) was dissolved in DMF (7.5 ml). The mixture was stirred at 60 °C for 3 h. Then, the reaction was quenched with water, and the mixture was extracted with ethyl acetate. The organic layers were combined, washed with water and then bine, dried over $MgSO_4$ and concentrated under vacuum. The residue was purified by preparative TLC and then recrystallized from petroleum ether (60–90) to afford **23–29**.

23. Yield: 38.7%, white solid; ^{1}H NMR (500 MHz, $CDCl_3$) δ 7.61 (d, J = 7.6 Hz, 1H), 7.54 (d, J = 6.9 Hz, 1H), 7.48–7.39 (m, 1H), 7.28 (d, J = 12.8 Hz, 1H), 7.21 (t, J = 8.2 Hz, 1H), 7.13 (d, J = 8.4 Hz, 1H), 6.98 (d, J = 8.4 Hz, 1H), 4.27 (d, J = 6.6 Hz, 1H), 4.10 (d, J = 14.3 Hz, 1H), 3.97 (dd, J = 28.0, 16.2 Hz, 2H), 3.70–3.61 (m, 1H), 3.53 (dd, J = 14.3, 7.4 Hz, 1H), 3.34–3.22 (m, 1H), 2.37–2.25 (m, 1H), 1.79–1.67 (m, 1H), 1.01 (d, J = 6.5 Hz, 3H); ^{13}C NMR (151 MHz, DMSO-d_6) δ: 163.07, 161.45, 147.74, 145.32, 143.47, 132.19, 128.55, 123.22, 120.31, 120.17, 115.72, 114.20, 114.04, 110.32, 51.64, 48.74, 44.03, 42.56, 34.69, 17.81; HRMS (ESI (+)) m/z calculated for $C_{19}H_{19}ClN_3O_3S$ $[M + H]^+$: 424.0892, found 424.0891.

24. Yield: 44.7%, white solid; ^{1}H NMR (500 MHz, $CDCl_3$) δ 7.74 (d, J = 7.4 Hz, 2H), 7.28 (s, 1H), 7.13 (d, J = 8.3 Hz, 1H), 6.97 (d, J = 8.2 Hz, 1H), 6.89 (d, J = 7.4 Hz, 2H), 4.25 (d, J = 6.5 Hz, 1H), 4.05 (d, J = 14.5 Hz, 1H), 3.95 (d, J = 14.8 Hz, 2H), 3.80 (s, 3H), 3.63 (dd, J = 13.5, 11.1 Hz, 1H), 3.51 (dd, J = 14.3, 7.7 Hz, 1H), 3.30–3.19 (m, 1H), 2.32–2.17 (m, 1H), 1.73 (s, 1H), 1.01 (d, J = 6.3 Hz, 3H); ^{13}C NMR (151 MHz, DMSO-d_6) δ: 163.06, 162.73, 147.73, 145.36, 133.08, 129.17, 128.55, 120.13, 115.67, 114.84, 110.29, 55.97, 51.11, 48.62, 43.93, 42.14, 36.23, 34.66, 31.25, 17.87; HRMS (ESI (+)) m/z calculated for $C_{20}H_{22}ClN_3O_4S$ $[M + H]^+$: 436.1092, found 436.1091.

25. Yield: 45.0%, white solid; ^{1}H NMR (500 MHz, $CDCl_3$) δ 7.82 (d, J = 7.8 Hz, 2H), 7.59–7.39 (m, 3H), 7.28 (s, 1H), 7.13 (d, J = 8.4 Hz, 1H), 6.97 (d, J = 8.4 Hz, 1H), 4.34–4.21 (m, 1H), 4.09 (d, J = 14.4 Hz, 1H), 3.98 (t, J = 15.5 Hz, 2H), 3.67–3.58 (m, 1H),

3.50 (dd, J = 14.5, 7.7 Hz, 1H), 3.33–3.20 (m, 1H), 2.37–2.21 (m, 1H), 1.74–1.68 (m, 1H), 1.00 (dd, J = 19.0, 6.7 Hz, 3H); ^{13}C NMR (151 MHz, DMSO-d_6) δ: 163.06, 147.75, 145.36, 141.39, 133.12, 129.82, 128.55, 126.97, 120.16, 115.71, 110.33, 51.40, 48.87, 44.07, 42.51, 34.80, 17.74; HRMS (ESI (+)) m/z calculated for $C_{19}H_{20}ClN_3O_3S$ $[M + H]^+$: 406.0987, found 406.0985.

26. Yield: 35.1%, white solid; ^{1}H NMR (600 MHz, $CDCl_3$) δ: 7.73 (d, J = 8.3 Hz, 2H), 7.45 (d, J = 7.4 Hz, 2H), 7.28 (d, J = 12.7 Hz, 2H), 7.13 (dd, J = 8.4, 1.3 Hz, 1H), 7.01–6.92 (m, 1H), 4.30–4.19 (m, 1H), 4.09 (d, J = 13.8 Hz, 1H), 3.96 (t, J = 15.0 Hz, 2H), 3.70–3.60 (m, 1H), 3.52 (dd, J = 11.8, 6.0 Hz, 1H), 3.31–3.20 (m, 1H), 2.31–2.16 (m, 1H), 1.73–1.63 (m, 1H), 1.31 (d, J = 17.1 Hz, 9H), 1.00 (d, J = 6.7 Hz, 3H); ^{13}C NMR (151 MHz, $CDCl_3$) δ: 162.51, 156.45, 147.42, 144.35, 138.13, 129.47, 126.71, 126.09, 120.40, 116.25, 109.24, 51.29, 49.59, 44.79, 43.59, 35.52, 35.07, 31.02, 18.21; HRMS (ESI (+)) m/z calculated for $C_{23}H_{28}ClN_3O_3S$ $[M + H]^+$: 462.1613, found 462.1609.

27. Yield: 33.2%, off-white solid; ^{1}H NMR (600 MHz, $CDCl_3$) δ: 7.31 (t, J = 7.5 Hz, 3H), 7.14 (d, J = 8.2 Hz, 1H), 6.98 (d, J = 6.8 Hz, 1H), 6.89 (d, J = 8.3 Hz, 1H), 4.24 (d, J = 14.8 Hz, 5H), 4.07 (d, J = 14.0 Hz, 1H), 4.03–3.90 (m, 2H), 3.64 (t, J = 11.5 Hz, 1H), 3.54 (s, 1H), 3.30–3.20 (m, 1H), 1.73–1.64 (m, 1H), 1.26 (s, 1H), 1.02 (d, J = 6.1 Hz, 3H); ^{13}C NMR (151 MHz, $CDCl_3$) δ: 162.36, 147.29, 143.98, 143.59, 133.73, 129.55, 120.55, 117.77, 116.43, 116.21, 109.30, 77.21, 77.00, 76.79, 64.46, 64.14, 51.25, 49.45, 44.84, 43.41, 35.45, 18.27; HRMS (ESI (+)) m/z calculated for $C_{21}H_{22}ClN_3O_5S$ $[M + H]^+$: 464.1041, found 464.1040.

28. Yield: 47.1%, white solid; ^{1}H NMR (500 MHz, $CDCl_3$) δ: 7.93 (t, J = 7.3 Hz, 1H), 7.53 (d, J = 4.8 Hz, 1H), 7.35–7.22 (m, 2H), 7.15 (dd, J = 11.6, 8.3 Hz, 2H), 6.97 (d, J = 8.4 Hz, 1H), 4.29–4.17 (m, 1H), 4.17–3.97 (m, 3H), 3.61 (t, J = 10.7 Hz, 2H), 3.47–3.33 (m, 1H), 2.40–2.26 (m, 1H), 1.73 (dd, J = 15.1, 7.5 Hz, 1H), 0.96 (d, J = 6.5 Hz, 3H); ^{13}C NMR (151 MHz, DMSO-d_6) δ: 163.09, 159.20, 157.52, 147.77, 145.36, 136.08, 130.58, 128.98, 128.56, 125.58, 120.17, 117.89, 117.75, 115.73, 110.34, 51.60, 49.17, 44.22, 42.79, 34.86, 17.64; HRMS (ESI (+)) m/z calculated for $C_{19}H_{19}ClFN_3O_3S$ $[M + H]^+$: 424.0892, found 424.0892.

29. Yield: 22.6%, off-white solid; ^{1}H NMR (600 MHz, $CDCl_3$) δ: 7.72 (d, J = 7.6 Hz, 2H), 7.66 (s, 1H), 7.58 (d, J = 7.3 Hz, 2H), 7.14 (d, J = 8.3 Hz, 1H), 6.99 (d, J = 6.6 Hz, 1H), 4.28 (d, J = 5.8 Hz, 1H), 4.05–3.86 (m, 3H), 3.68 (t, J = 10.7 Hz, 1H), 3.56 (d, J = 7.0 Hz, 1H), 3.31–3.20 (m, 1H), 2.30–2.12 (m, 5H), 1.75–1.63 (m, 1H), 1.02 (d, J = 5.7 Hz, 3H); ^{13}C NMR (151 MHz, $CDCl_3$) δ: 168.63, 161.95, 147.03, 141.95, 135.75, 129.74, 127.97, 120.87, 119.30, 115.99, 109.54, 51.25, 49.18, 44.83, 42.97, 35.10, 24.65, 18.26, 14.17; HRMS (ESI (+)) m/z calculated for $C_{21}H_{23}ClN_4O_4S$ $[M + H]^+$: 463.1201, found 463.1200.

Biological activity

For intracellular calcium measurements, Flp-In-CHO-OX1 and Flp-In-CHO-OX2 stable cells were grown in Ham's F-12K (Kaighn's modified Ham's F-12 Nutrient Mixture), 600 μg ml^{-1} hygromycin B, 10% fetal bovine serum and 1× penicillin–streptomycin (PS). The OX1R and OX2R cells were seeded into Corning black 384-well clear-bottom sterile plates at 6500 cells per well and 7000 cells per well, respectively. Fetal bovine serum, penicillin–streptomycin, HBSS (calcium and magnesium with no phenol red) and HEPES were obtained from Gibco, Ham's F-12K was obtained from HyClone, 1× PBS (pH 7.2–7.4) was obtained from Solarbio, 1× TrypLE express enzyme (no phenol red) was obtained from Thermo Fisher Scientific, and hygromycin B gold solution was obtained from Invivogen. The seeded plates were incubated overnight at 37 °C under 5% CO_2. Human orexin-A stock solution and test compound stock (30 nM) solutions were prepared. Human orexin-A solution was prepared by diluting the stock solution in assay buffer (1× HBSS and 20 mM HEPES) to a final concentration of 8 nM for use in the assay. The test compound solutions were prepared by diluting the stock solution. Then, the test compound solutions, DMSO and assay buffer were added into 384-well plates in order. The cells were washed with assay buffer and then incubated for 120 min at 37 °C in 40 μl of assay buffer containing 1× component A (calcium probe) and 2.5 mM of probenecid on the day of the assay. Test compound solutions (10 μl) were added to the plate and incubated for 30 min at rt. Then, 10 μl of the agonist was added. The intensity of the fluorescence was measured for each well at 1 s intervals for 2 min and compared with the intensity of the fluorescence induced by orexin-A (8 nM) instead of the antagonist. The IC_{50} value for each antagonist was determined.

Docking

DS software (www.3dsbiovia.com) was used for the docking studies. All the ligand structures were prepared by Gauss View 5.0 program. All the ligands were optimized using the Gaussian 09 program (www.gaussian.com) using the density functional theory (DFT) method at the B3LYP/6-311G (d,p) level. For protein preparation, the crystal structure coordinates of the human orexin receptor were obtained from the reference and then prepared with AutoDockTools 4.2 and PyMOL. The binding site coordinates of the receptors were determined by the size of the ligand in the PDB file (PDB 6TO7 and 6TPJ).[32] Docking simulations were performed using CDOCKER (for GABAAR) and LibDock (for CYP11B1) protocol in DS to predict how the ligands bind to OX1R and OX2R. The co-crystallized ligand (suvorexant) within the structures were defined as a center of the binding site. Generally, ten poses were generated for each docked ligand. Other docking options were kept as default. To validate the docking reliability, suvorexant was first re-docked to the binding site. Consequently, all ligands were docked into the same active site.

Conclusions

In this study, twenty one novel azacycloheptane sulfonamide derivatives were designed and synthesized, and all the compounds were evaluated as potential orexin receptor antagonists. Surprisingly, compound **23** showed high inhibitory activity against OX1R and OX2R, and the IC_{50} values of compound **23** against OX1R and OX2R were 0.63 μM and 0.17 μM, respectively. Moreover, compounds **19** and **24** exhibited potent inhibitory activities against OX1R *in vitro*. The binding

modes of suvorexant and compound **23** to OX2R indicated that the amino acid residues Asn324 and His350 were important for ligand binding *via* hydrogen bonding interactions, π–π stacking interactions, or π–σ interactions, which could explain the SAR of these compounds and is consistent with the active data. Hence, azacycloheptane sulfonamide derivatives are promising scaffolds for the discovery of novel OX1R and OX2R antagonists.

Conflicts of interest

There are no conflicts to declare.

Notes and references

1 T. Sakurai, A. Amemiya, M. Ishii, I. Matsuzaki, R. M. Chemelli, H. Tanaka, S. C. Williams, J. A. Richardson, G. P. Kozlowski, S. Wilson, J. R. S. Arch, R. E. Buckingham, A. C. Haynes, S. A. Carr, R. S. Annan, D. E. McNulty, W.-S. Liu, J. A. Terrett, N. A. Elshourbagy, D. J. Bergsma and M. Yanagisawa, *Cell*, 1998, **92**, 573–585.

2 L. de Lecea, T. S. Kilduff, C. Peyron, X.-B. Gao, P. E. Foye, P. E. Danielson, C. Fukuhara, E. L. F. Battenberg, V. T. Gautvik, F. S. Bartlett, W. N. Frankel, A. N. van den Pol, F. E. Bloom, K. M. Gautvik and J. G. Sutcliffe, *Proc. Natl. Acad. Sci. U. S. A.*, 1998, **95**, 322–327.

3 C. T. Beuckmann and M. Yanagisawa, *J. Mol. Med.*, 2002, **80**, 329–342.

4 C. Brisbare-Roch, J. Dingemanse, R. Koberstein, P. Hoever, H. Aissaoui, S. Flores, C. Mueller, O. Nayler, J. van Gerven, S. L. de Haas, P. Hess, C. Qiu, S. Buchmann, M. Scherz, T. Weller, W. Fischli, M. Clozel and F. Jenck, *Nat. Med.*, 2007, **13**, 150–155.

5 R. M. Chemelli, J. T. Willie, C. M. Sinton, J. K. Elmquist, T. Scammell, C. Lee, J. A. Richardson, S. C. Williams, Y. Xiong, Y. Kisanuki, T. E. Fitch, M. Nakazato, R. E. Hammer, C. B. Saper and M. Yanagisawa, *Cell*, 1999, **98**, 437–451.

6 J. T. Willie, R. M. Chemelli, C. M. Sinton, S. Tokita, S. C. Williams, Y. Y. Kisanuki, J. N. Marcus, C. Lee, J. K. Elmquist, K. A. Kohlmeier, C. S. Leonard, J. A. Richardson, R. E. Hammer and M. Yanagisawa, *Neuron*, 2003, **38**, 715–730.

7 M. A. Akanmu and K. Honda, *Brain Res.*, 2005, **1048**, 138–145.

8 C. Boss, C. Brisbare-Roch and F. Jenck, *J. Med. Chem.*, 2009, **52**, 891–903.

9 I. Banerjee, *Nepal J. Epidemiol.*, 2018, **8**, 713–715.

10 A. J. Roecker, C. D. Cox and P. J. Coleman, *J. Med. Chem.*, 2016, **59**, 504–530.

11 A. Kumar, P. Chanana and S. Choudhary, *Pharmacol. Rep.*, 2016, **68**, 231–242.

12 K. Janto, J. R. Prichard and S. Pusalavidyasagar, *J. Clin. Sleep Med.*, 2018, **14**, 1399–1408.

13 W. J. Herring, T. Roth, A. D. Krystal and D. Michelson, *J. Sleep Res.*, 2018, **28**, e12782.

14 R. A. Porter, W. N. Chan, S. Coulton, A. Johns, M. S. Hadley, K. Widdowson, J. C. Jerman, S. J. Brough, M. Coldwell, D. Smart, F. Jewitt, P. Jeffrey and N. Austin, *Bioorg. Med. Chem. Lett.*, 2001, **11**, 1907–1910.

15 C. J. Langmead, J. C. Jerman, S. J. Brough, C. Scott, R. A. Porter and H. J. Herdon, *Br. J. Pharmacol.*, 2004, **141**, 340–346.

16 M. A. Steiner, J. Gatfield, C. Brisbare-Roch, H. Dietrich, A. Treiber, F. Jenck and C. Boss, *ChemMedChem*, 2013, **8**, 898–903.

17 P. Malherbe, E. Borroni, L. Gobbi, H. Knust, M. Nettekoven, E. Pinard, O. Roche, M. Rogers-Evans, J. Wettstein and J.-L. Moreau, *Br. J. Pharmacol.*, 2009, **156**, 1326–1341.

18 B. A. Kummangal, D. Kumar and H. N. Mallick, *Behav. Brain Res.*, 2013, **237**, 59–62.

19 T. E. Fitch, M. J. Benvenga, C. D. Jesudason, C. Zink, A. B. Vandergriff, M. M. Menezes, D. A. Schober and L. M. Rorick-Kehn, *Front. Neurosci.*, 2014, **8**, 5.

20 A. J. Roecker, S. P. Mercer, J. D. Schreier, C. D. Cox, M. E. Fraley, J. T. Steen, W. Lemaire, J. G. Bruno, C. M. Harrell, S. L. Garson, A. L. Gotter, S. V. Fox, J. Stevens, P. L. Tannenbaum, T. Prueksaritanont, T. D. Cabalu, D. Cui, J. Stellabott, G. D. Hartman, S. D. Young, C. J. Winrow, J. J. Renger and P. J. Coleman, *ChemMedChem*, 2014, **9**, 311–322.

21 A. J. Roecker, T. S. Reger, M. C. Mattern, S. P. Mercer, J. M. Bergman, J. D. Schreier, R. V. Cube, C. D. Cox, D. Li, W. Lemaire, J. G. Bruno, C. M. Harrell, S. L. Garson, A. L. Gotter, S. V. Fox, J. Stevens, P. L. Tannenbaum, T. Prueksaritanont, T. D. Cabalu, D. Cui, J. Stellabott, G. D. Hartman, S. D. Young, C. J. Winrow, J. J. Renger and P. J. Coleman, *Bioorg. Med. Chem. Lett.*, 2014, **24**, 4884–4890.

22 S. Wu, Y. Sun, Y. Hu, H. Zhang, L. Hou, X. Liu, Y. Li, H. He, Z. Luo, Y. Chen, Y. Wang, W. Shi, L. Shen, C. Cao, W. Liang, Q. Xu, Q. Lv, J. Lan, J. Li and S. Chen, *Bioorg. Med. Chem. Lett.*, 2017, **27**, 1458–1462.

23 P. Malherbe, E. Borroni, E. Pinard, J. G. Wettstein and F. Knoflach, *Mol. Pharmacol.*, 2009, **76**, 618–631.

24 P. Hoever, S. de Haas, J. Winkler, R. C. Schoemaker, E. Chiossi, J. van Gerven and J. Dingemanse, *Clin. Pharmacol. Ther.*, 2010, **87**, 593–600.

25 C. D. Cox, M. J. Breslin, D. B. Whitman, J. D. Schreier, G. B. McGaughey, M. J. Bogusky, A. J. Roecker, S. P. Mercer, R. A. Bednar, W. Lemaire, J. G. Bruno, D. R. Reiss, C. M. Harrell, K. L. Murphy, S. L. Garson, S. M. Doran, T. Prueksaritanont, W. B. Anderson, C. Tang, S. Roller, T. D. Cabalu, D. Cui, G. D. Hartman, S. D. Young, K. S. Koblan, C. J. Winrow, J. J. Renger and P. J. Coleman, *J. Med. Chem.*, 2010, **53**, 5320–5332.

26 W. J. Herring, E. Snyder, K. Budd, J. Hutzelmann, D. Snavely, K. Liu, C. Lines, T. Roth and D. Michelson, *Neurology*, 2012, **79**, 2265–2274.

27 Y. Yoshida, T. Terauchi, Y. Naoe, Y. Kazuta, F. Ozaki, C. T. Beuckmann, M. Nakagawa, M. Suzuki, I. Kushida, O. Takenaka, T. Ueno and M. Yonaga, *Bioorg. Med. Chem.*, 2014, **22**, 6071–6088.

28 Y. Yoshida, Y. Naoe, T. Terauchi, F. Ozaki, T. Doko, A. Takemura, T. Tanaka, K. Sorimachi, C. T. Beuckmann,

M. Suzuki, T. Ueno, S. Ozaki and M. Yonaga, *J. Med. Chem.*, 2015, **58**, 4648–4664.

29 P. Murphy, M. Moline, D. Mayleben, R. Rosenberg, G. Zammit, K. Pinner, S. Dhadda, Q. Hong, L. Giorgi and A. Satlin, *J. Clin. Sleep Med.*, 2017, **13**, 1289–1299.

30 Y. Chen, Y. Zhou, J.-H. Li, J.-Q. Sun and G.-S. Zhang, *Chin. Chem. Lett.*, 2015, **26**, 103–107.

31 M. McKiernan, J. Huck, J. A. Fehrentz, M. L. Roumestant, P. Viallefont and J. Martinez, *J. Org. Chem.*, 2001, **66**, 6541–6544.

32 M. Rappas, A. A. E. Ali, K. A. Bennett, *et al.*, Comparison of Orexin 1 and Orexin 2 Ligand Binding Modes Using X-ray Crystallography and Computational Analysis, *J. Med. Chem.*, 2020, **63**, 1528–1543.